Asian Journal of Chemistry; Vol. 24, No. 7 (2012), 3174-3176

ASIAN JOURNAL OF CHEMISTRY

www.asianjournalofchemistry.co.in

Optimization of a Long Wavelength Vertical-Cavity Surface-Emitting Lasers by Employing Photonic Crystal

SAEID MARJANI[1,*] and HAMID MARJANI[2]

[1]Young Researchers Club, Arak Branch, Islamic Azad University, Arak, Iran
[2]Department of Electrical Engineering, Arak Branch, Islamic Azad University, Arak, Iran

*Corresponding author: E-mail: saeidmarjani@yahoo.com

(*Received*: 5 August 2011; *Accepted*: 18 February 2012) AJC-11093

In this work, we attempt to design, simulate and characterize a GaAs-based high power long wavelength vertical-cavity surface-emitting lasers by employing combined single defect photonic crystal index guiding layer and oxide layer. In this way, increases the optical wavelength from 1.541 μm to 1.568 μm and the lasing power 85.382 % from 11.349 mW to 21.039 mW at a bias current of 35 mA. The device employs InGaAsP active region, which is sandwiched between GaAs/AlGaAs and GaAs/AlAs distributed Bragg reflectors. The basic design goal was to obtain vertical-cavity surface-emitting laser with the high power, high slop efficiency for L-band optical fiber application. This paper provides key results of the device characteristics, including the optical wavelength, the output power and threshold current.

Key Words: Optimization, Long wavelength, Photonic crystal, Vertical-cavity surface-emitting laser.

INTRODUCTION

A crystal is a periodic arrangement of atoms or molecules. The pattern which the atoms or molecules are repeated in space is the crystal lattice. The crystal presents a periodical potential to an electron propagating through it and both the constituents of the crystal and the geometry of the lattice dictate the conduction properties of the crystal. If the dielectric constants of the materials in the crystal are sufficiently different and if the absorption of light by the materials is minimum, then the refractions and reflections of light from all the different interfaces can present many of the same phenomena for photons that the atomic potential produces for electrons.

Fig. 1 is a schematic representation of several three-dimensional lattices of spheres in a cubic cell. The simplest lattice is formed by the blue spheres at the corners of the cube. If we add the dark red spheres at the centers of the faces, we obtain a face-centered cubic (or fcc) lattice. The fcc lattice vectors are (ˆx + ˆy)a/2, (ˆy + ˆz) a/2 and (ˆx + ˆz)a/2. Finally, if we add the pink spheres, which represent another fcc lattice that is shifted by (a/4, a/4, a/4) relative to the blue spheres, then we obtain a diamond lattice[1].

In recent years, the characteristics of vertical cavity surface emitting laser (VCSEL) have extremely improved[2]. Vertical cavity surface emitting lasers are important light sources in optical communication systems where single mode, high output power and low threshold current are desirable for certain applications[3]. Vertical cavity surface emitting laser devices developed using the wafer fusion method have achieved continuous wave lasing at wavelength of 1550 nm at power, threshold voltage and current about 0.65 mW, 2.5 V and 1 mA respectively[4]. TU Berlin researchers have also produced 1530 nm vertical cavity surface emitting lasers capable of 40 Gbit/sec modulation, based on indium phosphide technology[5].

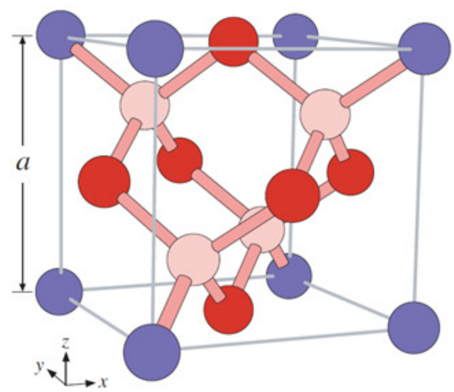

Fig. 1. Ball-and-stick (atomic) representation of several three-dimensional lattices in a cubic supercell, with a lattice constant a. The blue balls alone form a simple cubic lattice. Adding the dark red balls produces a face-centered cubic (fcc) lattice. Adding the pink balls as well produces a diamond lattice, with stick bonds (four bonds per ball)

In this paper, we design a high power InGaAsP vertical cavity surface emitting laser by employing combined single defect photonic crystal index guiding layer and oxide layer for L-band optical fiber application. In the following, we first describe the numerical model. Next the simulated vertical cavity surface emitting laser structures are introduced. Finally, the conclusions provide common guidelines for designing performance of vertical cavity surface emitting lasers.

EXPERIMENTAL

In modeling vertical cavity surface emitting lasers, we must consider the electrical, optical and thermal interaction during laser performance. Thus base of simulation is to solve Poisson and continuity equations for electrons and holes[6]. Poisson's equation is defined by:

$$\nabla.(\varepsilon\nabla\psi) = \rho \tag{1}$$

where, ψ is electrostatic potential, ρ is local charge density and ε is local permittivity. The continuity equations of electron and hole are given by[7]:

$$\frac{dn}{dt} = G_n - R_n + \frac{1}{q}\nabla.j_n \tag{2}$$

$$\frac{dp}{dt} = G_p - R_p + \frac{1}{q}\nabla.j_p \tag{3}$$

where, n and p are the electron and hole concentration, J_n and J_p are the electron and hole current densities, G_n and G_p are the generation rates for electrons and holes, R_n and R_p are the recombination rates and q is the magnitude of electron charge.

The fundamental semiconductor equations (1)-(3) are solved self-consistently together with Helmholtz and the photon rate equations. The applied technique for solution of Helmholtz equation is based on improved effective index model[8], which shows accuracy for great portion of preliminary problems. This model is very good adapted to simulation of laser structures and it is often called effective frequency method[9].

Two-dimensional Helmholtz equation is solved to determine the transverse optical field profile and it is given by[6]:

$$\nabla^2 E(r,z,\varphi) + \frac{\omega_0}{c^2}\varepsilon(r,z,\varphi,\omega)E(r,z,\varphi) = 0 \tag{4}$$

where, ω is the frequency, $\varepsilon(r, z, \varphi, \omega)$ is the complex dielectric permittivity, $E(r, z, \varphi)$ is the optical electric field and c is the speed of light in vacuum. The light power equation relates electrical and optical models. The photon rate equation is given by[6]:

$$\frac{dS_m}{dt} = \left(\frac{c}{N_{eff}}G_m - \frac{1}{\tau_{ph_m}} - \frac{cL}{N_{eff}}\right)S_m + R_{sp_m} \tag{5}$$

where, S_m is the photon number, G_m is the modal gain, R_{spm} is the modal spontaneous emission rate, L represents the losses in the laser, N_{eff} is the group effective refractive index, τ_{phm} is the modal photon lifetime and c is the speed of light in vacuum.

Equations (1)-(5) provide an approach that can account for the mutual dependence of electrical, thermal, optical and elements of heat sources. In this paper, we employ numerical-based simulation software to assist in the device design and optimization[6].

Fig. 2 shows the schematic structures of vertical cavity surface emitting laser device, which are used for simulation. The vertical cavity surface emitting laser device consists of an active region of six $In_{0.76}Ga_{0.24}As_{0.82}P_{0.18}$ quantum wells and seven $In_{0.48}Ga_{0.52}As_{0.82}P_{0.18}$ barriers, bounded between 30 periods of top and 28 periods of bottom DBR mirrors. The top one is $GaAs/Al_{0.33}Ga_{0.67}As$ with index of refraction of layers 3.38 and 3.05, respectively and the bottom one is GaAs/AlAs with index of refraction of layers 3.38 and 2.89, respectively. The incorporation of a high aluminum content layer ($Al_{0.98}Ga_{0.02}As$) in two DBR periods above the active region allows for selective oxidation.

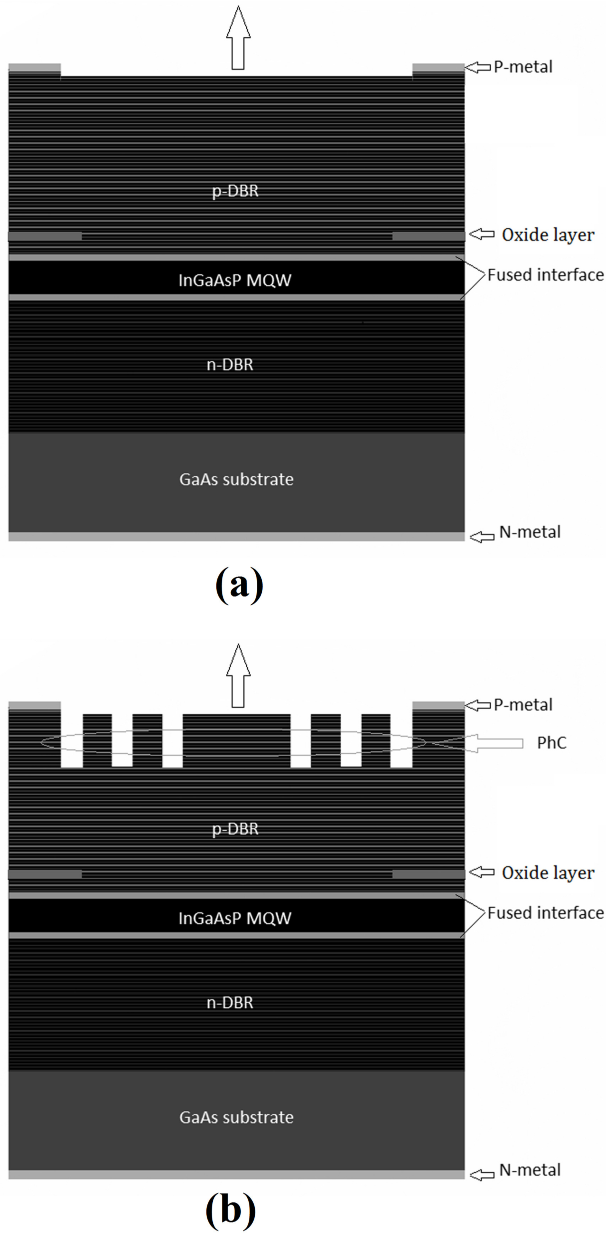

Fig. 2. Schematic structure of the laser devices (a) Simple vertical cavity surface emitting laser (b) PhC vertical cavity surface emitting laser

In order to investigate the dependence of the characteristics of vertical cavity surface emitting lasers on the photonic crystal, vertical cavity surface emitting lasers with the following two types of structures were simulated; a) Simple vertical cavity surface emitting laser, as shown in Fig. 2a; b) Vertical cavity surface emitting laser modified by photonic crystal as shown in Fig. 2b. Triangular-lattice air holes are formed in the upper pairs of top distributed Brag reflectors. The optical confinement is achieved by means of seven air holes where the center is missed off to make the defect region.

RESULTS AND DISCUSSION

Fig. 3 shows the output power characteristics for the vertical cavity surface emitting lasers with various structures. The output powers of structure (a) and (b) are 11.349 mW and 21.039 mW at a bias current of 35 mA, respectively. The difference of these output powers arises from the different the hole etching on the top distributed Bragg reflectors, which have better confined the optical field within a single defect of the photonic crystal. As can be seen from Fig. 3, structure (b) increased slope of power versus current curve than structure (a), which is mainly related to the reduction of the mode volume. The threshold current of structure (a) and (b) are 1.128 mA and 4.162 mA, respectively. Such parasitic effect is related to the leakage of the light through the photonic crystal holes since the holes are too shallow (2 μm) to confine efficiently the mode.

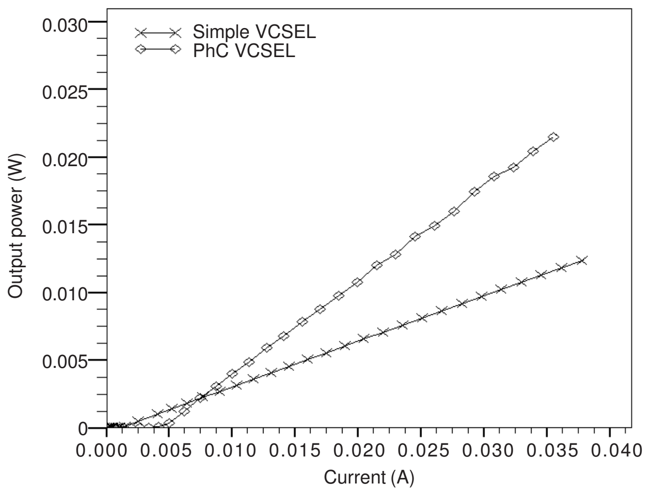

Fig. 3. Output power characteristics for the vertical cavity surface emitting lasers (VCSELs) with various structures

Fig. 4 shows the optical wavelength for the vertical cavity surface emitting lasers with various structures. At higher currents, the optical wavelength of structure (a) and (b) are 1.541 μm and 1.568 μm, respectively. This increment should be mainly due to etching on the top distributed Bragg reflectors.

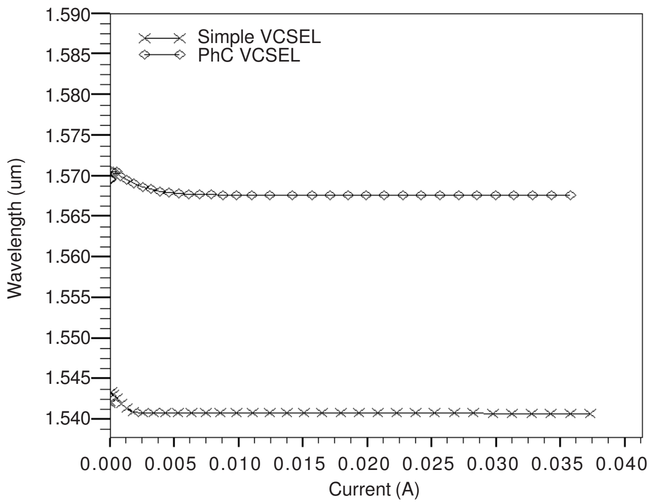

Fig. 4. Optical wavelength for the vertical cavity surface emitting lasers (VCSELs) with various structures

Conclusion

A new structure of a GaAs-based long wavelength vertical-cavity surface-emitting lasers (LW VCSELs) was designed for L-band optical fiber application. We have successfully increased the optical wavelength from 1.541 μm to 1.568 μm and the lasing power 85.382 % from 11.349 mW to 21.039 mW at a bias current of 35 mA.

REFERENCES

1. J.D. Joannopoulos, S.G. Johnson, R.D. Meade and J.N. Winn, Photonic Crystals: Molding the Flow of Light, Princeton, University Press, edn. 2, pp. 94-99 (2008).
2. K. Iga, *IEEE J. Select. Topics Electron.*, **6**, 1201 (2000).
3. I.-S. Chung and J. Moerk, In Proceedings of 11th International Conference on Transparent Optical Networks, ICTON '09, IEEE, The Azores, Portugal, pp.1-4 (2009).
4. A. Karim, J. Piprek, P. Abraham, D. Lofgreen, Y.-J. Chiu and J.E. Bowers, *IEEE J. Sel. Topics Quantum Electron.*, **7**, 178 (2001).
5. W. Hofmann, M. Mueller, P. Wolf, A. Mutig, T. Gruendl, G. Boehm, D. Bimberg and M.C. Amann, *Electron. Lett.*, **47**, 270 (2011).
6. Silvaco International, Atlas User's Manual, USA, Silvaco International Incorporated (2010).
7. J. Piprek, Semiconductor Optoelectronic Devices: Introduction to Physics and Simulation, Ch. 3 Carrier Transport and Ch. 6 Heat Generation and Dissipation UCSB: Academic Press, pp. 49-50 and pp. 141-147 (2003).
8. G.R. Hadley, *J. Opt. Lett.*, **20**, 1483 (1995).
9. H. Wenzel and H.J. Wunsche, *IEEE J. Quantum Electron.*, **33**, 1156 (1997).